CrossMark

A novel hydrogel based on agricultural waste for removal of hazardous dyes from aqueous solution and reuse process in a secondary adsorption

Ghada A. Mahmoud[1] · **Samia E. Abdel-Aal**[1] ·
Nagwa A. Badway[2] · **A. A. Elbayaa**[2] · **Doaa. F. Ahmed**[2]

Abstract A novel hydrogel based on the orange peel (OP) and *N*-vinyl-2-pyrrolidone was prepared by free-radical polymerization using gamma irradiation. The effect of radiation dose and hydrogel composition on gel content was studied. The formed hydrogel was characterized by FT-IR, TGA, and SEM. The swelling behavior was determined as a function of swelling time, pH, and OP content. The hydrogel swelling was found to be pH dependent, and the diffusion mechanism of water into the hydrogel was found Fickian. The developed hydrogel was used for the removal of Congo red (CR) and methyl orange (MO) dyes from wastewater. The effects of various operating parameters, such as initial pH, contact time, initial dye concentration, and temperature on the removal of dyes, have been investigated. The Langmuir and the Freundlich adsorption models were applied to study the adsorption isotherm. The pseudo-first-order model was proved compatible for CR adsorption and the pseudo-second-order model well described the adsorption of MO. The adsorption of dyes increased with increasing temperature indicating that the endothermic nature of the adsorption process and the thermodynamic parameters was evaluated. Second, the adsorption cycle of dyes was also examined and discussed utilizing the loaded hydrogel with the other dye and cobalt metal ions.

Keywords Agricultural waste · Dye removal · Hydrogel · Radiation · Second adsorption

✉ Ghada A. Mahmoud
  ghadancrrt@yahoo.com

1   National Center for Radiation Research and Technology, Atomic Energy Authority,
    P.O. Box 29, Nasr City, Cairo, Egypt

2   Chemistry Department, Faculty of Science, Al-Azhar University, Nasr City, Cairo, Egypt

🙋 Springer

Introduction

Dyes are synthetic chemical compounds having complex aromatic structures which are extensively used in the textile, cosmetic, plastic, food, and pharmaceutical industries [1]. Most of dyes can cause damage not only to aquatic life but also to human beings, because they are toxic, mutagenic, or carcinogenic [2]. Various methods are used for the removal of dyes from wastewater, such as adsorption, coagulation, advanced oxidation, and membrane separation. Adsorption is one of the most effective processes of advanced wastewater treatment employed to reduce hazardous pollutants present in the effluent [3]. Researchers contributed largely to find low-cost adsorbents with greater adsorption capacities that can remove dyes from the effluent, such as agricultural waste based on their unique advantages; nontoxic, biocompatible, biodegradable, inexpensive, and abundant [4]. One of the important agricultural wastes is the peel of different fruits, which can serve as potential adsorbents for the removal of diverse types of pollutants [5]. Orange peel (OP) mainly consists of cellulose, pectin, hemicelluloses lignin, chlorophyll, pigment, and other low molecular weight hydrocarbons [6], and it has been used to remove dyes from wastewaters [7, 8]. However, it is prone to enzymatic degradation and suffers from limitations in fabrication [9]. Copolymerization is a technique, which improves the properties of natural polymers and gives them a new property [10]. Copolymers offer advantages not usually seen in homopolymers. For this reason, many of the absorbable polymers are of the copolymer type [11].

Hydrogel is polymeric cross-linked network structures [12], and it describes three-dimensional network structures obtained from a class of synthetic and/or natural polymers which can absorb and retain a significant amount of water [13]. Therefore, many studies focused on the use of hydrogels as an adsorbent to remove dyes particularly that contain functional groups, such as carboxylic acid, amine, and sulfonic acid groups [14–16].

The use of ionizing radiation for the preparation of hydrogels offers some advantages over the conventional methods, including; no need for cross-linking agents or initiators to initiate the reaction, and the cross-linking reaction may be initiated at ambient temperature [17]. The degree of crosslinking strongly affects the properties of hydrogels that may be controlled by varying the irradiation dose [18].

In this study, a hydrogel based on orange peel (OP) waste copolymerized with *N*-vinyl-2-pyrrolidone (NVP) as a synthetic monomer, for a first time, by gamma irradiation technique. Incorporating this natural waste with a synthetic polymer showed the synergistic effect on the functionalities and properties of this hybrid system. Characterization and properties of the produced (NVP/OP) hydrogels were investigated. The prepared hydrogel served as an adsorbent for the removal of Congo red (CR) and methyl orange (MO) dyes from aqueous solutions. The dye-loaded hydrogels were alternatively used to remove the other dye as a second adsorption cycle.

Materials and methods

Materials

Orange peel was collected from the local area in the winter season. Reagent grade N-vinyl-2-pyrrolidone (NVP) purity 99 % (Merck, Germany) (Fig. 1) was used as received. The other chemicals, such as dyes, were reagent grade and used without further purification (Fig. 1).

Orange peel treatment

Orange peels were washed thoroughly with distilled water to remove the adhering dirt. The washed peels were left to dry in sunlight to evaporate moisture for 72 h, then crushed. The ground powder was treated with 1 % sodium hydroxide and ethanol to remove lignin and pigments. Orange peel was then filtered out, washed with distilled water to remove free sodium hydroxide and dried in the air.

Synthesis of hydrogel

A 10 g of OP was placed in 100 mL distilled water, stirred, and heated at 80 °C for 120 min to form a homogeneous mixture, then cooled to room temperature, and different contents of NVP monomers were added and continuously stirred at room temperature for 5 min. The solutions were transferred into glass tubes to irradiate with the Co^{60} gamma source at different radiation doses (10–50 kGy) at a dose rate of 1.46 kGy/h. After irradiation, the cross-linked NVP/OP hydrogel was purified by washing in excess water, so that unreacted chemicals were leached out, then air dried at room temperature.

To determine the insoluble part in the hydrogel, the hydrogel samples were air dried to a constant weight. The dried samples were soaked in distilled water for 24 h
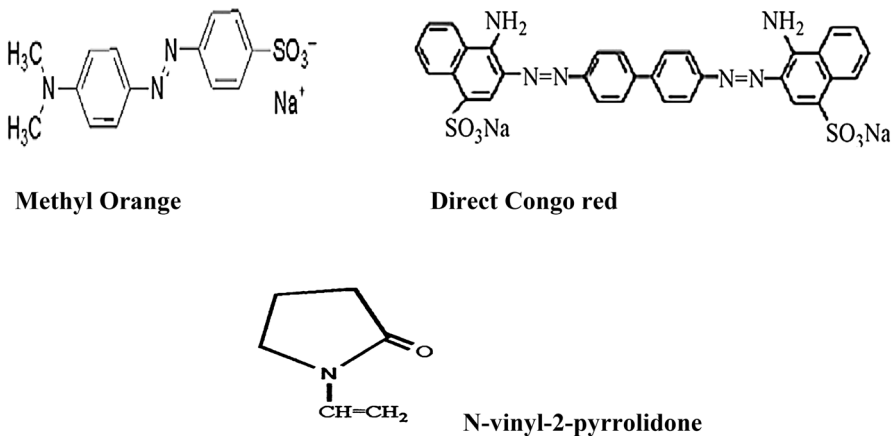

Fig. 1 Chemical structure of methyl orange, direct congo red, and N-vinyl-2-pyrrolidone

at 70 °C, then taken out and washed with hot water to remove the soluble part and dried to a constant weight. The gel content was calculated gravimetrically applying the following formula:

$$\text{Gel content } (\%) = \frac{W_d}{W_0} \times 100 \tag{1}$$

where W_d and W_0 are the dried sample weights after and before extraction, respectively.

The swelling measurements

The clean, dried, weighed hydrogel was soaked in bi-distilled water at room temperature for different time intervals. The sample was then removed, and the excess water on the surface was removed by blotting quickly with filter paper and reweighed. The swelling percent was calculated as follows:

$$\text{Swelling } (\%) = \frac{W_s - W_d}{W_d} \times 100 \tag{2}$$

where W_d and W_s are the masses of dry and swelled hydrogel, respectively.

To investigate the swelling behavior at various pH values, the samples were allowed to swell in several pH solutions at room temperature in a similar way. The pH values were adjusted by the addition of 0.1 M NaOH or 0.1 M HCl solution to a designed value.

Characterization of hydrogel

The functional groups of the synthesized hydrogel were characterized by FT-IR spectra recorded on Nicolet IS-10FTIR, within the range 400–4000 cm^{-1} using KBr pellets.

To study the morphology of the hydrogel, the scanning electron micrographs were recorded using JEOL-JSM-5400 scanning electron microscope, Tokyo, Japan. Before the examination, the materials were dried, coated with sputtered gold, observed, and photographed.

The thermal properties of the hydrogel were investigated using Shimadzu, Japan; TGA system of type TGA-50 under the nitrogen atmosphere (20 mL/min). The temperature ranged from ambient to 600 °C at a heating rate of 10 °C/min. The primary TGA thermograms were used to determine the rate of the thermal decomposition reaction.

Adsorption study

Batch adsorption experiments were carried out at different temperatures that ranged between 20 and 60 °C. Exactly 20 mL of dye solution of known initial concentration (10–50 mg/L) at adjusted pH was shaken at a certain agitation speed

of 250 rpm with a known dose of dried hydrogel for appropriate time intervals. The percentage removal of dye was calculated using the following equation:

$$\text{Removal } (\%) = \frac{C_0 - C_t}{C_0} \times 100 \tag{3}$$

where C_0 and C_t (both in mg/L) are the initial dye concentration and the dye concentration at time t, respectively.

The adsorption capacity q_e (mg/g) at equilibrium was calculated using the following equation:

$$q_e = \frac{(C_i - C_e)}{W} \times V \tag{4}$$

where V is the solution volume (L), W is the weight of hydrogel sample (g), and C_i and C_e are the initial and final (or equilibrium) dye concentrations (mg/L), respectively. The concentration of CR and MO was determined by using a UV/VIS spectrometer, model UV-Analytic Jena AG, and made by German that was used at $\lambda_{\max}$ of 500 nm for CR and 464 nm for MO with a quartz cell of 1.0 cm optical length.

Results and discussion

Gel content

Figure 2 shows the gelation percent of (NVP/OP) hydrogels as a function of radiation dose at different hydrogel compositions. The gel fraction increased rapidly
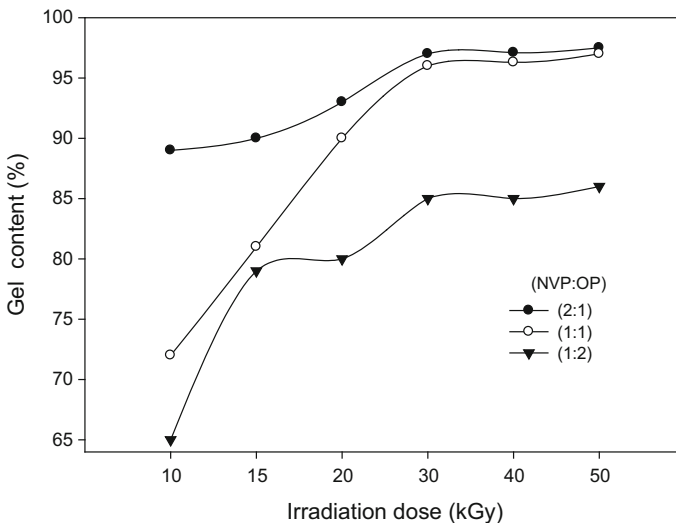

Fig. 2 Effect of irradiation dose on the gel fraction of different hydrogel compositions

by increasing radiation dose from 10 up to 30 kGy, beyond which a slight increase in the gel fraction was observed up to 50 kGy. When an aqueous solution of NVP and OP was irradiated with gamma-rays, free radicals were generated on the polymer chains and monomers by the indirect effect of radicals generated by radiolysis of water. Random reactions of these radicals caused polymerization and formation of a network. An increase in the total radiation dose enhances the formation of radicals in the reaction mixture which causes a high degree of crosslinking and thus high gel content of hydrogel [19]. As radiation dose increased beyond a certain value (30 kGy), the polymer chains crosslinked and a gel was obtained. Therefore, the optimum radiation dose for the preparation of (NVP/OP) hydrogel was 30 kGy. The capacity of forming a gel is also affected by the hydrogel composition. It is clear that the gel content in the hydrogel increased with increasing NVP content, because the hydrogel structure becomes dense; with higher cross-linking density. In other words, the gel content decreased with increasing OP content, because the main chain scission is the predominant reaction and low probability of the recombination of the degraded OP chains.

(NVP/OP) hydrogel properties and characterization

The swelling behavior of a hydrogel is greatly influenced by factors, such as radiation dose, copolymer composition, swelling time, and the pH of the swelling medium.

Figure 3 shows the effect of swelling time on the swelling percent of (NVP/OP) hydrogel at different irradiation doses. The swelling capacity of the hydrogels increased with the swelling time and reached the state of equilibrium after 24 h. As shown in Fig. 3, the swelling percent decreases with increasing dose due to an increase in crosslinking and hence a decreasing in the swelling percent.
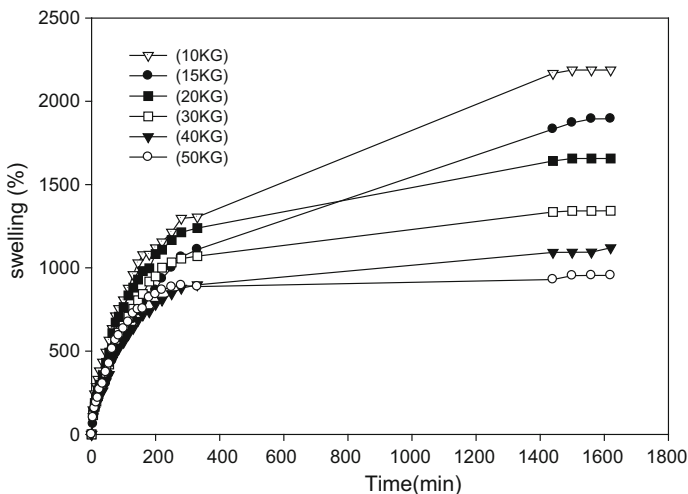

Fig. 3 Effect of time on the swelling percent of (NVP/OP) (1:1) hydrogel at different irradiation doses

The diffusion of the water into a hydrogel depends on both the physical properties of the hydrogel network and the interactions between the hydrogel and the water itself [20]. To decide the nature of water diffusion mechanism into (NVP/OP) hydrogels, the swelling data with time were fit with the Fickian diffusion equation according to the following [21]:

$$F = kt^n \tag{5}$$

$$\ln F = \ln k + n \ln t \tag{6}$$

where F is the fraction of water uptake at time t, n is the diffusional exponent, which is indicative of the transport mechanism, and k is a constant incorporating characteristics of the polymeric network system. The above equation is valid for the first 60 % of the normalized solvent uptake.

The nature of the solvent diffusion process is classified according to the value of n, Fickian, non-Fickian diffusions, or Super Case II models. When the value of $n \leq 0.5$, the mechanism is Fickian, which is characterized by a solvent diffusion rate, and is slower than the polymer relaxation, where the sorption is diffusion controlled, whereas, when $n = 1$, relaxation control occurs, leading to the zero-order release. When the value of n is between 0.5 and 1, the release follows non-Fickian diffusion which is characterized by the solvent diffusion rate and the polymer relaxation are about the same order of magnitude, where the system will be diffusion and relaxation controlled [22]. Plots of $\ln F$ versus $\ln t$ were plotted at various radiation doses (S1), and values of n and k were calculated from the slope and intercept of the lines, respectively, and the data are listed in Table 1. All the values of n were found to be lower than 0.5, and hence the diffusion of water into the applied hydrogels was of Fickian character; this means that the diffusion of water controls the swelling.

Figure 4 represents the TGA and the rate of thermal decomposition (dw/dt) curves of two compositions of (NVP/OP) hydrogel at temperatures ranged from 25 up to 600 °C. Three characteristic stages of decomposition were observed, the first decomposition stage within the temperature range 29–130 °C can be ascribed to the vaporization of physically absorbed water. The second decomposition stage is between 130 and 400 °C can be examined on the basis of anhydride formation and degradation of the intermolecular side chain. The main weight loss occurs in the third step within the range 400–475 °C which may be attributed to the decomposition of the backbone polymer. A very little change in the thermal

Table 1 Fikian parameters of (NVP/OP) hydrogel at different radiation doses

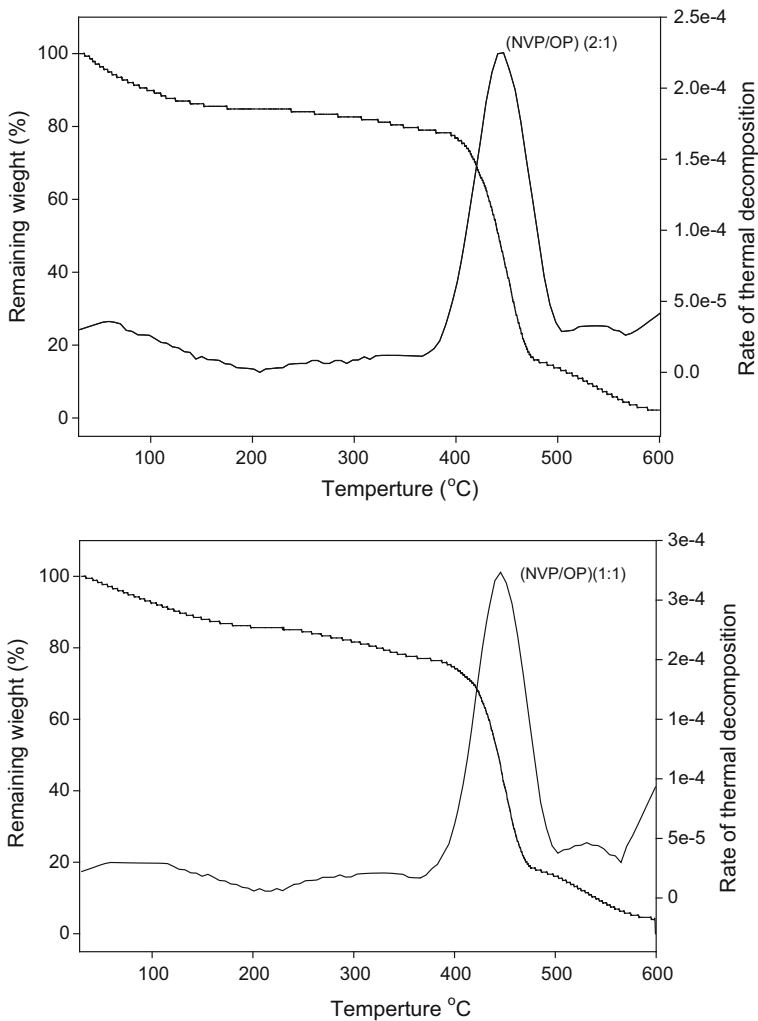| Irradiation dose (kGy)	n	$\ln k$	k	R^2
10	0.43	−2.9	0.05	0.993
15	0.49	−3.3	0.04	0.992
20	0.46	−2.9	0.05	0.987
30	0.45	−2.7	0.07	0.986
40	0.42	−2.5	0.08	0.985
50	0.43	−2.3	0.09	0.982

Fig. 4 TGA and decomposition rate for (NVP/OP) hydrogel of different compositions at irradiation dose (30 kGy)

stability was observed as a resulted increasing the NVP content in the hydrogel. It can be concluded that the prepared hydrogel (NVP/OP), at sample proportions, is mostly stable up to temperature 200 °C which is suitable for some applications. The surface scanning of the two different hydrogel compositions was confirmed using SEM, as shown in Fig. 5. It can be observed that both (NVP/OP) hydrogels of composition (2:1) and (1:1) had a coarse surface with irregular cavities of large dimensions. The (NVP/OP) hydrogel of composition (1:1) had more and larger pores than that of composition (2:1). The presence of pores plays an important role in the hydrogel swelling capacity, hence, in the adsorption capacity. The dye
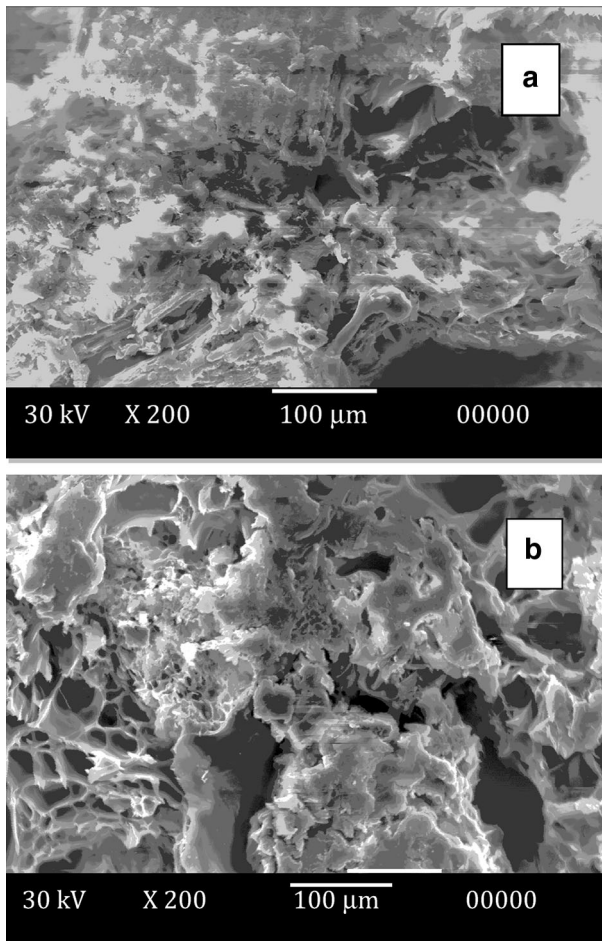
Fig. 5 SEM of (NVP/OP) hydrogel of composition (2:1) (**a**) and (1:1) (**b**) at irradiation dose (30 kGy)

molecules can interact easily with the functional groups on the external surface of the hydrogel.

Adsorption study

In this part, the adsorption properties of the prepared NVP/OP hydrogel towards Congo red (CR) and methyl orange (MO) dyes are investigated. The hydrogel composition taken was (NVP/OP) (1:1) at the radiation dose of 30 kGy which was given the most homogeneity and suitable properties for the practical application. Factors affecting the adsorption properties, such as treatment time, pH, initial dye concentration, and temperature, are evaluated.

The effect of pH on the adsorption of CR and MO dyes onto NVP/OP hydrogel was examined, and the results are presented in Fig. 6. The adsorption capacity was
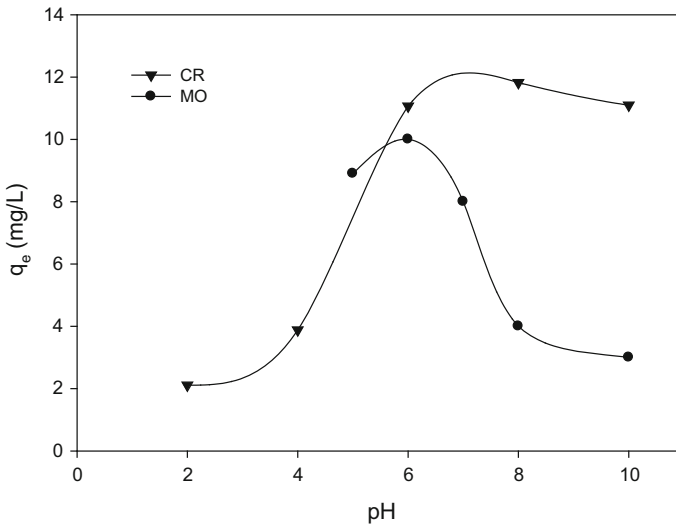
Fig. 6 Effect of pH on the adsorption capacity of CR and MO dyes at ambient temperature and initial concentration 25 mg/L

examined over a range of pH values between 2 through 10 for CR and 5 through 10 for MO, where the dye precipitated at pH lower than 5, so the result could not be detected. It was found that the adsorption capacity of CR was increased with the increase in pH of the dye solution and the maximum value was reached at pH = 7, but further increase in pH caused a slight reduction in the adsorption capacity. Solution pH would affect both adsorbate chemistry and surface binding sites of the adsorbents [23]. At neutral pH levels, hydrophobic interactions between a hydrophobic modified natural polymer tail and hydrophobic CR moieties, and the solution was most stable at this pH. At elevated initial pH values, a decrease in adsorption value could be interpreted by enhancing the formation of OH ions that competing with the dye anionic species for the adsorption sites [24]. For the adsorption of MO adsorption onto (NVP/OP) hydrogel, it was found that an increase in adsorption capacity was observed with the increase in pH from 5 up to 6 and further increase in pH led to a decrease in MO adsorption, Fig. 5. At pH 6, MO occurs as a quinoid form in aqueous system predominating dispersion interaction process. Further increase in pH led to a decrease in MO adsorption. A similar behavior for MO adsorption on different adsorbents was reported elsewhere [25]. Therefore, further adsorption experiments were carried out at pH = 7 for the adsorption of CR dye and at pH = 6 for the adsorption of MO dye.

Contact time studies are helpful in understanding the amount of dye adsorbed at various time intervals by a fixed amount of the adsorbent. The adsorption process proceeds in several steps involving transport of the solute from solution to the surface of the solid particles and diffusion of the solute into the interior of the pores which is usually a slow process [26]. The adsorbed amount of CR and MO onto (NVP/OP) hydrogel versus contact time at the initial dye concentration 10 (mg/L)

was investigated, and the results are presented in Fig. 7. The increase of contact time led to the increase in the amount of dye adsorbed, and the equilibrium was reached at 6000 and 4000 min for CR and MO, respectively. As adsorption continues, the functional groups of the fixed amount of hydrogel present in the aqueous medium become exhaust, thus the rate of adsorption decreases. Finally, it reaches a dynamic equilibrium when the rate of adsorption by the hydrogel equals the rate of desorption from the hydrogel clearly indicates a rapid increase in the amount of adsorption with an increase in time initially, gradually leading to equilibrium [27].
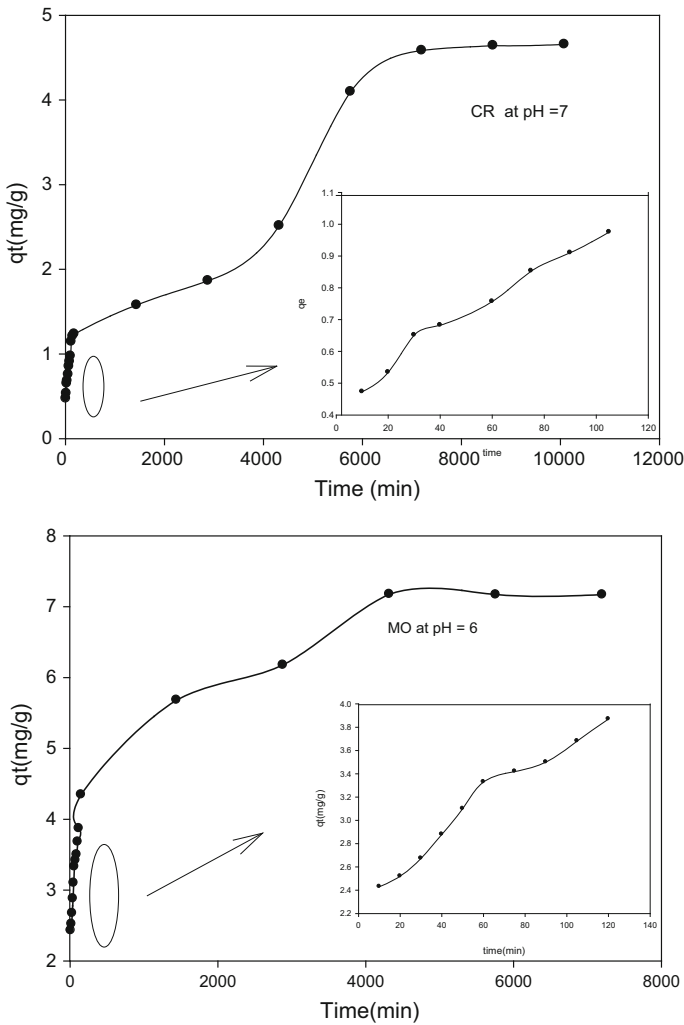

Fig. 7 Effect of contact time on the adsorption capacity of CR and MO dyes at ambient temperature and initial concentration 10 mg/L

To investigate the mechanism of adsorption, the behavior of the dyes adsorption process was analyzed using the pseudo-first order [28] and the pseudo-second order [29]. In the pseudo-first-order model, the adsorption rate is expected to be proportional to the first power of concentration, where the adsorption is characterized by diffusion through a boundary. The pseudo-first-order model sometimes does not fit well for the whole range of contact time when it failed theoretically to predict the amount of dye adsorbed and thus deviated from the theory. In that case, the pseudo-second-order model is based on the sorption capacity of the solid phase, where the pseudo-second-order model assumes that chemisorptions may be the rate-controlling step in the adsorption processes [30].

The pseudo-first-order and the pseudo-second-order models are as follows:

Pseudo-first-order model

$$\log(q_e - q_t) = \log q_e - \frac{k_1}{2.303} t \tag{7}$$

Pseudo-second-order model

$$\frac{t}{q_t} = \frac{1}{k_2 q_e^2} + \frac{1}{q_e} t \tag{8}$$

where q_e and q_t are the amounts of dye adsorbed (mg/g) at equilibrium and at time t, respectively, k_1 (min^{-1}) is the pseudo-first-order rate constant, and k_2 (g/mg/min) is the pseudo-second-order rate constant. k_1 is calculated by plotting log $(q_e - q_t)$ vs t and k_2 are calculated by plotting t/q_t vs t (S2). The characteristic parameters of the studied kinetic models and their corresponding correlation coefficients are presented in Table 2. Predicting from the correlation coefficients, for CR and MO, the pseudo-first-order model has higher correlation coefficient ($R^2 \approx 0.97$) compared to the correlation coefficient of the pseudo-second order ($R^2 \approx 0.95$). Obviously, the adsorption of CR dye can be well described by the pseudo-first-order adsorption mechanism. For MO dye, the correlation coefficient of the pseudo-second-order model has higher correlation coefficient ($R^2 \approx 0.99$) compared to the correlation coefficient for the pseudo-first-order ($R^2 \approx 0.98$). Thus, the adsorption of MO can be well described by the pseudo-second-order adsorption mechanism, and hence, the adsorption rate of MO is probably controlled by chemical process [31].

Table 2 Pseudo-first-order and the pseudo-second-order parameters for the adsorption of CR and MO dyes

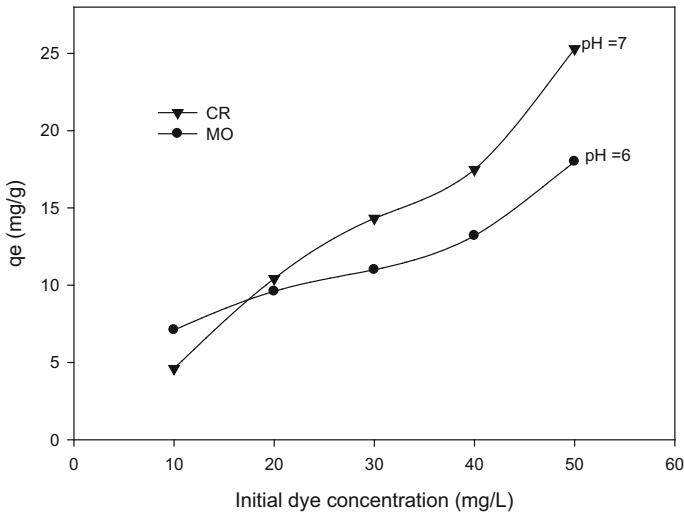| Model	Parameters	CR values	MO values
Pseudo-first order	$q_{e,\mathrm{exp}}$ (mg/g)	4.60	7.10
	$q_{e,\mathrm{cal}}$ (mg/g)	4.21	5.65
	k_1 (min^{-1})	0.124	2.7×10^{-3}
	R^2	0.95	0.98
Pseudo-second order	k_2 (g mg/min)	0.0165	0.0169
	$q_{e,\ \mathrm{cal}}$ (mg/g)	1.48	4.16
	R^2	0.97	0.99

Fig. 8 Effect of initial dye concentration on the adsorption capacity of CR and MO dyes at ambient temperature and contact time 24 h

Figure 8 shows the effect of the initial dye concentration on the dye adsorption capacity of (NVP/OP) hydrogel by varying the dye concentrations between 10 and 50 mg/L. It can be noted that dye adsorption increased with the increase in dye concentration; i.e., increases in the initial dye concentration enhance the interaction between adsorbent and dye molecules [32]. Namely, the adsorption capacity increased from 4.8 to 26.0 mg/g for CR and from 4.6 to 10.0 mg/g for MO when the initial dye concentration increased from 10 to 50 mg/L, respectively. This may be

Table 3 Comparison of the adsorption capacities of CR and MO dyes on various biomass-based adsorbents

Adsorbent	q_e (mg/g)	References
CR dye		
(NVP/OP)	26	This study
Poly(*N*-vinyl-2pyrrolidone)	Not available	[28]
Orange peel	11.4	[20]
Tamarind fruit shell	3.84	[29]
Bottom ash	2.05	[30]
Deoiled soya	15,5	[30]
Activated coir pitch carbon	6.72	[31]
Cashew nut shell	5.18	[23]
Mo dye		
(NVP/OP)	10	This study
Poly(*N*-vinyl-2pyrrolidone)	Not available	[33]
Orange peel	15.4	[30]
Bottom ash	3.6	[34]

due to the high driving force of mass transfer at higher initial dye concentration [33]. The resistance to mass transfer between the solid and aqueous phase more easily overcomes the driving forces; moreover, increasing the number of collisions between dye molecules and adsorbent resulted in increasing the adsorption capacity. A comparison of the maximum adsorption capacity (q_e) values of CR and MO onto (NVP/OP) to some natural adsorbents in the literature is shown in Table 3. It can be seen that NVP itself is unable for the adsorption of CR and MO dye and the adsorption capacity of OP towards CR is far lower than the adsorption capacity of the investigated (NVP/OP) hydrogel towards these dyes.

To discuss the adsorption isotherm, two commonly used models are investigated; the Langmuir and the Freundlich models. The Langmuir model [34] represents a monolayer sorption process onto a homogenous surface and can be written as:

$$\frac{C_e}{q_e} = \frac{C_e}{q_{max}} + \frac{1}{b \cdot q_{max}} \tag{9}$$

where q_{max} is maximum adsorption capacity (mg/g), C_e is equilibrium dye concentration in solution (mg/L), and b is Langmuir constant (L/mg).

The Freundlich model [35] is applied to describe a heterogeneous system characterized by a heterogeneity factor of $1/n$. This model describes reversible adsorption and is not restricted to the formation of the monolayer and can be written as:

$$\log q_e = \log K_F + \frac{1}{n} \log C_e \tag{10}$$

where K_F is the Freundlich isotherm constant, and $1/n$ is the heterogeneity factor.

The two isotherm models were plotted (S3), and the parameters were evaluated and summarized in Table 4. According to the correlation coefficient (R^2), the Freundlich model provided a better linearity than the Langmuir model for both CR and MO dyes which indicated that the Freundlich isotherm correctly fits the equilibrium data and the values of n are more than one, i.e., the adsorption intensity is favorable. This means that the sorption of CR and MO onto NVP/OP hydrogel is of heterogeneous energy distribution.

The essential characteristics of the Langmuir model to show the feasibility of the Langmuir isotherm can be explained in terms of the separation factor (R_L). It can be expressed by the following equation [26]:

Table 4 Parameters of the Langmuir and the Freundlich isotherm models

Model	Parameters	CR	MO
Langmuir	q_m (mg/g)	75	8.9
	k_a (L/mg)	0.03	0.02
	R_L	0.61	0.49
	R^2	0.85	0.94
Freundlich	K_F [mg g $(L/g)^{-1/n}$]	2.40	3.07
	n	3.80	1.14
	R^2	0.99	0.96

$$R_{\text{L}} = \frac{1}{(1 + nC_0)} \tag{11}$$

where C_{o} (mg/L) is the initial concentration. The value of R_{L} indicates the adsorption is favorable or unfavorable. If the value of R_{L} higher than 1 means the unfavorable adsorption, if the value of R_{L} between zero and 1 means the favorable adsorption, while $R_{\text{L}} = 1$ means the linear adsorption and $R_{\text{L}} = 0$ means the irreversible adsorption. As shown in Table 4, the values of R_{L} lie between 0 and 1 confirmed the favorable adsorption of CR and MO onto (NVP/OP) hydrogel.

The relationship between the temperature variation and the adsorption capacity of CR and MO by NVP/OP hydrogel was investigated and shown in Fig. 9. The adsorption capacity increased as temperature elevated from 20 to 60 °C, i.e., the mobility of dye ions was accelerated with temperature. The mobile number of species acquires the sufficient energy to undergo interactions with active sites at the surface, and the adsorption is an endothermic reaction.

The thermodynamic parameters, such as Gibb's free energy (ΔG^{o}), enthalpy change (ΔH^{o}), and entropy change (ΔS^{o}), for the adsorption of CR and MO dyes onto (NVP/OP) hydrogel can be calculated by the following equations [36]:

$$\Delta G^o = -RT\ln k_c \tag{12}$$

$$\Delta G^o = \Delta H^{\text{o}} - T\Delta S^{\text{o}} \tag{13}$$

$$K_c = C_a/C_e \tag{14}$$

where C_a and C_e are the equilibrium dye concentration (mg/L) on the adsorbent and in the solution, respectively, R is the universal gas constant (8.314 J/mol/K), and
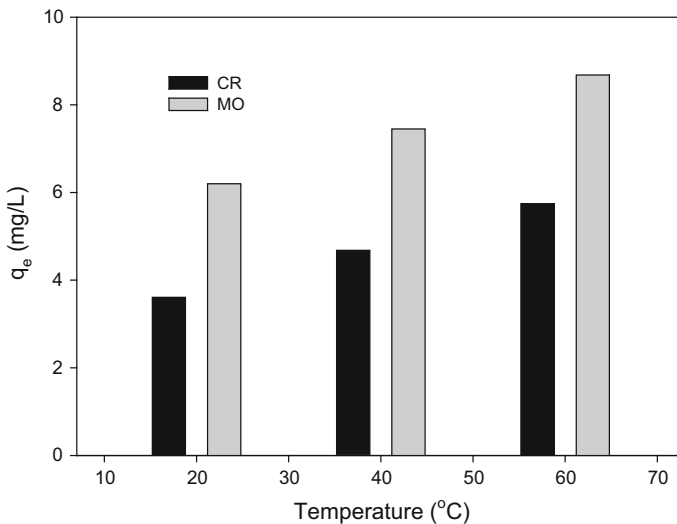

Fig. 9 Effect of temperature on the adsorption capacity of CR and MO dyes onto (NVP/OP) hydrogel at the initial dye concentration 10 mg/L

Table 5 Thermodynamic parameters of CR and MO dyes onto (NVP/OP) hydrogel	Temp (K)	ΔH^0 (kJ/mol)		ΔS^0 (J/mol)		ΔG^o (kJ/mol)	
		CR	MO	CR	MO	CR	MO
	293					−5.33	−6.01
	313	2.577	4.156	18.20	20.53	−5.69	−6.42
	333					−6.05	−6.83

T is absolute temperature (K). The values of ΔH^o and ΔS^o were calculated, respectively, from the slope and intercept of plot between ln K_c versus $1/T$ (S4), and the results are listed in Table 5. The positive values of ΔH^o confirm the endothermic nature of adsorption. It is also observed that the enthalpy change in the range 20–40 kJ/mol indicates the physisorption adsorption of dyes at the three experimental temperatures. The negative values of ΔG^o imply the spontaneous nature of the adsorption process. Furthermore, the decrease in the negativity of ΔG^o values with rising temperature indicates that the adsorption is more spontaneous at higher temperatures. The positive value of ΔS^o suggests increasing the randomness at the solid–solution interface.

FT-IR analysis

The FT-IR spectra of the free- and dye-loaded (NVP/OP) hydrogel are shown in Fig. 10. OP mainly consists of celluloses, hemicelluloses, pectin, lignin, and many other low molecular weight compounds that play an important part in biosorption [37]. The spectrum of (NVP/OP) hydrogel shows a broadband at 3452.49 cm^{-1} corresponding to the (O–H) stretching vibrations of alcohol, phenol, and carboxylic acid group in pectin, cellulose, and lignin, respectively, and confirms the presence of "free" hydroxyl groups on the adsorbent surface as components of the OP [38]. The bands at 2953 and 2891 cm^{-1} correspond to the asymmetric and symmetric C–H stretching vibration of CH$_2$ groups, respectively, in the cellulose of OP or aliphatic C–H in (NVP). The band at 1661.51 cm^{-1} is due to C=O stretching vibration of the cyclic amide of (NVP). The band at 1495 cm^{-1} indicates COO$^-$ (asymmetric) and C–C stretching in the aromatic compound of lignin, and the band at 1463 cm^{-1} indicated CH$_3$ of lignin. The C–N bending and stretching of (NVP) appear at 1425 and 1289 cm^{-1}, respectively, and the stretching vibration of –SO$_3$ of hemicelluloses appears at 1373 cm^{-1}. The bands in region 1200–1025 cm^{-1} are due to C–O and C–O–C stretching vibrations.

For (NVP/OP)-CR, the broad stretching band of –OH is shifted to 3474 cm^{-1} indicating the intra-molecular hydrogen bonding between (OP/NVP) hydrogel chains and the dye molecules. The C–H and C=O stretching bands are shifted to 2880 and 1658.86 cm^{-1}, respectively. For (NVP/OP)-MO, the O–H stretching band shifted to 3451.2 cm^{-1}, C–H stretching band shifted to 2880 cm^{-1}, and C=O shifted to 1658.86 cm^{-1}.
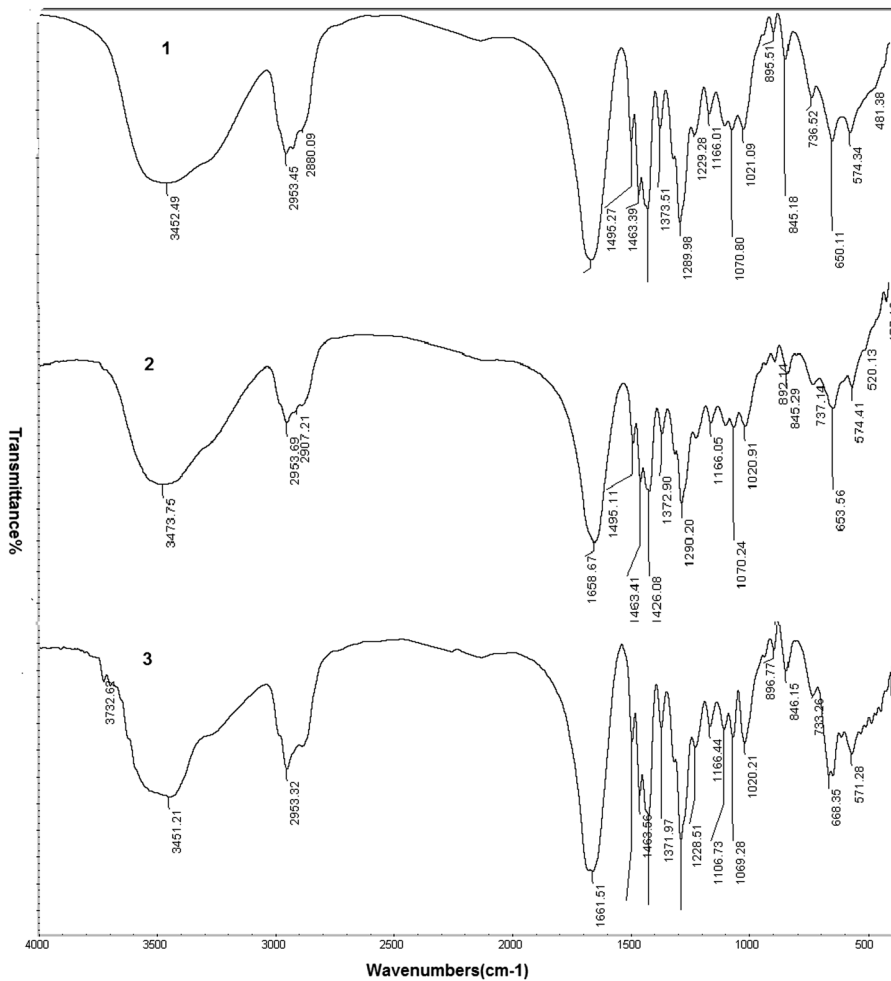
Fig. 10 FT-IR spectra of (OP/NVP) (1:1) (*1*), (OP/NVP)/CR (*2*) and (OP/NVP)/MO (*3*)

Second adsorption cycle of (NVP/OP) hydrogel

A very important factor for developing an adsorbent in practical applications is the reuse of adsorbent. The traditional treatment for the used adsorbent was to wash and recover for recycle use. Recently, a novel way to make use of these used adsorbents has been reported in the literature [39]. Since the surface structure of adsorbents has been changed after being covered by a layer of contaminant, the used hydrogel can be applied to adsorb other pollutants at suitable conditions. The adsorption of MO and CR as a second adsorption cycle onto (NVP/OP)/CR and (NVP/OP)/MO, respectively, was examined as a function of time at pH = 7 to avoid desorption of dye and shown in Fig. 11. It can be observed that as the contact time increases, the removal percent also increases up to equilibrium. Good results were obtained in the
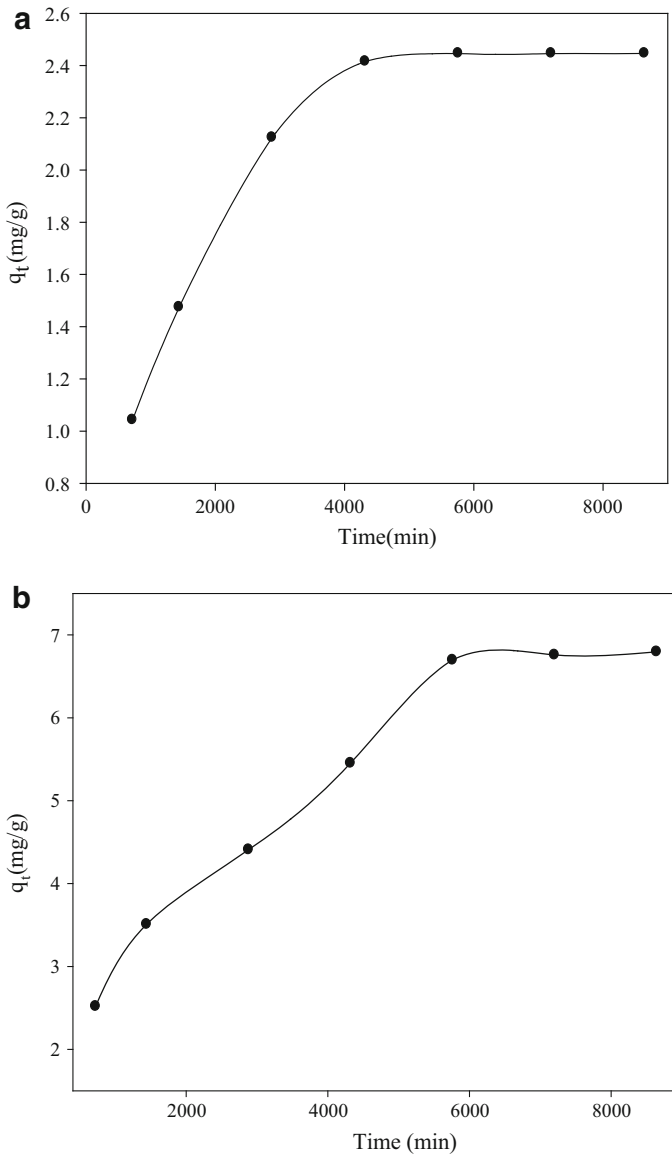
Fig. 11 Effect of contact time on adsorption CR by (NVP/OP)/MO (**a**) and MO by (NVP/OP)/CR (**b**) at the initial concentration 10 mg/L and pH 7

second adsorption of (NVP/OP)/MO and (NVP/OP)/CR. In this case, the adsorbent was covered with a layer of dye, which could adsorb part of other type of dye through electrostatic interaction [40].

On the other hand, the adsorption of CR and Mo onto (NVP/OP) loaded with Co (II) ions of concentration 10 mg/L was investigated as a function of time, and the
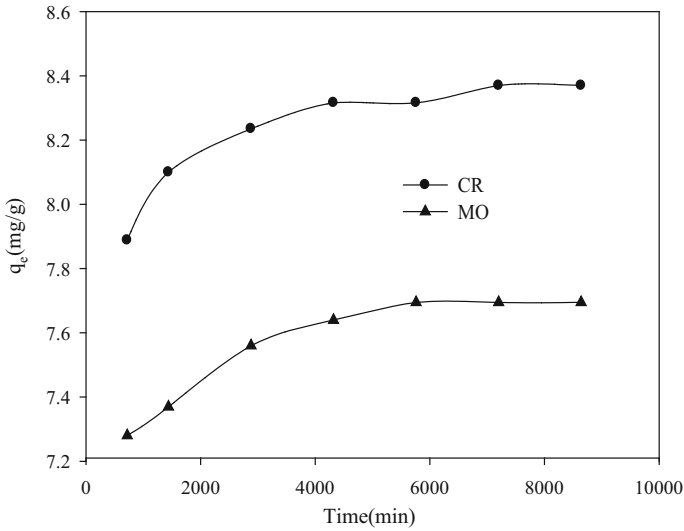
Fig. 12 Effect of contact time on adsorption CR by (NVP/OP)/Co (*a*) and MO by (NVP/OP)/Co (*b*) at the initial concentration 10 mg/L and pH 7

result is shown in Fig. 12. Improvement in the dye adsorption onto (NVP/OP) loaded Co (II) was observed particularly the adsorption of MO dye. This may be due to a formation of a complex between cobalt ions and dye molecules.

The surface morphology of (NVP/OP) hydrogel after the first and the second adsorption cycles was investigated and shown in Fig. 13a–f. The surface morphology was completely changed after adsorption compared with Fig. 5b. As shown in Fig. 13a, for the (NVP/OP) hydrogel surface after adsorption of MO, the pores were reduced as an evidence of adsorption. While the surface of (NVP/OP)/MO after a second adsorption cycle of CR (Fig. 13b) appeared as shallow forest. The (NVP/OP) hydrogel surface after the adsorption of CR (Fig. 13c) was depicted as herb texture with some cavities that reduced after the second adsorption cycle with MO and the surface appeared as a hay. The surface morphology of (NVP/OP) loaded with Co (II) ions after adsorption of MO and CR, as shown in (Fig. 13d, e), respectively, was appeared as coarse with bright spots.

Conclusions

The (NVP/OP) hydrogel was prepared using gamma radiation. The gel fraction increased by increasing the radiation dose and NVP content in the hydrogel. It was found that the swelling percent decreased as the radiation dose increased. The prepared hydrogel was mostly stable up to temperature 200 °C which is suitable for variant applications. The (NVP/OP) hydrogel was successfully evaluated for the adsorption of CR and MO dyes from their waste water. The maximum removal occurred at pH = 7 for CR and at pH = 6 for MO. The equilibrium data were well
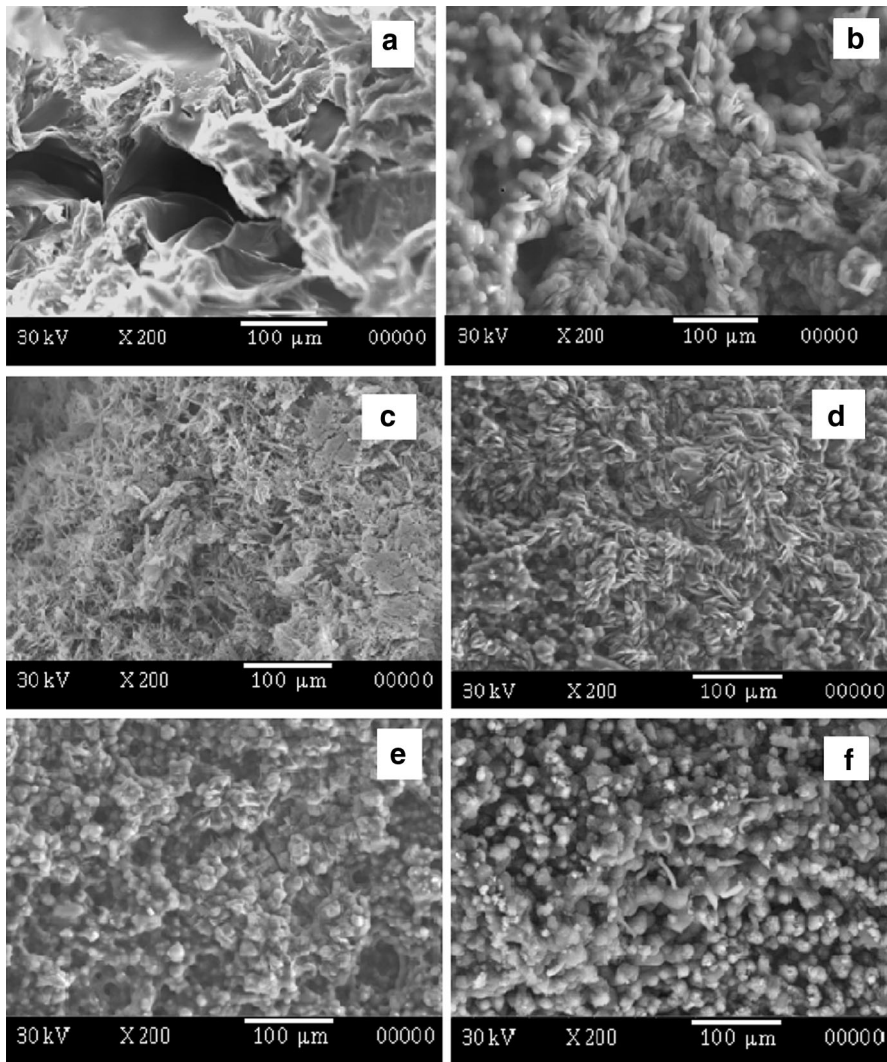
Fig. 13 SEM of (NVP/OP) loaded MO (**a**), (NVP/OP)/MO) loaded CR (**b**), (NVP/OP) loaded CR (**c**), (NVP/OP)/CR) loaded MO (**d**), (NVP/OP)/Co (II)) loaded Mo (**e**), and loaded CR (**f**)

analyzed using the Freundlich model. The pseudo-first-order model fits well the adsorption of CR, and the pseudo-second-order model described well the adsorption of MO. Thermodynamic parameters' values reflected the spontaneous and endothermic nature of the dyes adsorption by the hydrogel. Good results were obtained for employing (NVP/OP)/CR to remove (MO) as a second adsorption cycle and (NVP/OP)/MO to remove (CR) from aqueous solutions. Improvement in the dye adsorption onto (NVP/OP) loaded Co (II) was observed particularly adsorption of MO dye. Thus, the second adsorption is an efficient and economical way for reuse of the (NVP/OP) hydrogel.

References

1. Taleb AM, Hegazy DE, Mahmoud GA (2014) Characterization and in vitro drug release behavior of (2-hydroxyethyl methacrylate)–co-(2-acrylamido-2-methyl-1-propanesulfonic acid) crosslinked hydrogels prepared by ionizing radiation. Int J Polym Mater Polym Biomater 63:840–845

2. Guven OS, Karada E, Saraydın D (1999) the radiation synthesis of copolymeric hydrogels for adsorption and separation purposes. Radiat Phys Chem 56(3):81–386

3. Mohamed M, Olgun G (2012) Radiation-grafted copolymers for separation and purification purposes: status, challenges and future directions. Polym Sci 37:1597–1656

4. Mane VS, Babu PV (2013) Kinetic and equilibrium studies on the removal of Congo red from aqueous solution using Eucalyptus wood (*Eucalyptus globulus*) saw dust. J Taiwan Inst Chem E 44:81–88

5. Gong R, Ding Y, Yang C, Liu H, Sun Y (2005) Utilization of powdered peanut hull as biosorbent for removal of anionic dyes from aqueous solution. Dye Pigment 64:187–192

6. Vishakh K, Kishor B, Sudh R (2012) Natural polymers—a comprehensive review. Int J Res Pharm Biomed Sci (IJAPBS) 3:1597–1613

7. Pathak PD, Mandavgane SA, Kulkarni BD (2015) Fruit peel waste as a novel low-cost bio adsorbent. Rev Chem Eng 31(4):361–381

8. Titi OA, Bello OS (2015) An overview of low cost adsorbents for copper (II) ions removal. J Biotechnol Biomater 5(1):1–13

9. Liang S, Guo XY, Feng NC, Tian QH (2009) Adsorption of Cu^{2+} from aqueous solution by Mg^{2+}/K^+ type orange peel adsorbent. J Hazard Mater 174(1–3):756–762

10. Kumar KV, Porkodi K (2002) Batch adsorber design for different solution volume/adsorbent mass ratios using the experimental equilibrium data with fixed solution volume/adsorbent mass ratio of malachite green onto orange peel. Dyes Pigm 74:590–594

11. Mohamed SF, Mahmoud GA, Abou Taleb MF (2013) Synthesis and characterization of poly(acrylic acid)-g-sodium alginate hydrogel initiated by gamma irradiation for controlled release of chlortetracycline HCl. Monatsh Chem 144:129–137

12. Mahmoud GA, El-kelesh NA, Badway NA, Kamal FH, Abdel Aziz AM (2014) Characterisation of alginate-based nanocomposites prepared by radiation for removal of pesticides. Int J Nanoparticles 7(3/4):213–230

13. Kanagaraj J, Panda RC, Sumathi V (2015) Synthesis of graft-copolymer adsorbent through green route and studies on its interactions with chromium (III) through active functional groups: kinetics and improved adsorption supported by SEM-EDX and AFM. RSC Adv. doi:10.1039/C5RA05799J

14. Wang J, Li J (2015) One-pot synthesis of IPN hydrogels with enhanced mechanical strength for synergistic adsorption of basic dyes. Soft Mater 13:160–166

15. Dragan ES, Lazar MM, Dinu MV, Doroftei F (2012) Macroporous composite IPN hydrogels based on poly(acrylamide) and chitosan with tuned swelling and sorption of cationic dyes. Chem Eng J 204–206:198–209

16. Akkaya MÇ, Emik S, Güçlü G, İyim TB, Özgümüş S (2009) Removal of basic dyes from aqueous solutions by crosslinked-acrylic acid/acrylamidopropane sulfonic acid hydrogels. 114(2):1150–1159

17. Rosiak JM, Yoshii F (1999) Hydrogels and their medical applications. Nucl Instrum Methods Phys Res B 151:56–64

18. Yagub MT, Sen TK, Afroze S, Ang HM (2014) Dye and its removal from aqueous solution by adsorption: a review. Adv Colloid Interface Sci 209:172–184

19. Chen KS, Ku YA, Lin HR (2005) Preparation and characterization of pH sensitive poly(N-vinyl-2-pyrrolidone/itaconic acid) copolymerhydrogels). Mater Chem Phys 91:484–489

20. Ritger P, Peppas N (1987) A simple equation for description of solute release I. Fickian and non-fickian release from nonswellable devices in the form of slabs, spheres, cylinders or discs. J Control Release 5:23–36

21. Karadag E, Uzum OB, Saraydın D, Guven O (2006) Swelling characterization of gamma-radiation induced crosslinked acrylamide/maleic acid hydrogels in urea solutions. Mater Design 27:576–584

22. Luo Y, Peng Y, Wu Sun J, Wang Y (2011) Novel amphoteric pH-sensitive hydrogels derived from ethylenediaminetetraacetic dianhydride, butanediamine and amino-terminated poly(ethylene glycol): design, synthesis and swelling behavior. Eur Polym J 47:40–47

23. Annadurai G, Juang R, Lee D (2002) Use of cellulose-based wastes for adsorption of dyes from aqueous solutions. J Hazard Mater B 92:263–274

24. Chatterjee S, Lee DS, Lee MW, Woo SH (2009) Congo red adsorption from aqueous solutions by using chitosan hydrogel beads impregnated with nonionic or anionic surfactant. Bioresour Technol 100(17):3862–3868

25. Mohammadi N, Khani H, Amereh E, Agarwal S (2011) Adsorption process of methyl orange dye onto mesoporous carbon material-kinetic and thermodynamic studies. J Colloid Interface Sci. 362:457–462

26. Cheah W, Hosseini S, Khan MA, Chuah TG, Choong TSY (2013) Acid modified carbon coated monolith for methyl orange adsorption. Chem Eng J 215–216:747–754

27. Peng Q, Liu M, Zheng J, Zhou C (2015) Adsorption of dyes in aqueous solutions by chitosan–halloysite nanotubes composite hydrogel beads. Micropor Mesopor Mat 201:190–201

28. Lagergren S (1898) Zur theorie der sogenannten adsorption geloster stoffe. Kungliga Svenska Vetenskapsakademiens. Handlingar 24:1–39

29. Ho YS, McKay G, Wase DAJ, Foster CF (2000) Study of the sorption of divalentmetalions on to peat. Adsorpt Sci Technol 18:639–650

30. Crini G, Badot PM (2008) Application of chitosan, a natural aminopolysaccharide, for dye removal from aqueous solutions by adsorption processes using batch studies: a review of recent literature. Prog Polym 33:135–143

31. Mahmoud GA, Mohamed SF (2012) Removal of lead ions from aqueous solution using (sodium alginate/itaconic acid) hydrogel prepared by gamma radiation. Aust J Basic Appl Sci 6(6):262–272

32. Dawood S, Sen TK (2012) Removal of anionic dye Congo red from aqueous solution by raw pine and acid-treated pine cone powder as adsorbent: equilibrium, hermodynamic, kinetics, mechanism and process design. Water Res 461(1933–1):946

33. Bulut Y, Aydin H (2006) A kinetics and thermodynamics study of methylene blue adsorption on wheat shells. Desalination 194:259–267

34. Langmuir I (1916) The constitution and fundamental properties of solids and liquids. J Am Chem Soc 38:2221–2295

35. Freundlich HMF (1906) Uber die adsorption in losungen. Z Phys Chem 57:385–470

36. Anirudhan TS, Radhakrishnan PG (2008) Thermodynamics and kineticsof adsorption of Cu (II) from aqueous solution onto a new cation exchange derived from tamarind fruit shell. J Chem Thermodyn 40:702–709

37. Marín AB, Aguilar MI, Meseguer VF, Ortuno JF, Sáez J, Lloréns M (2009) Biosorption of chromium (III) by orange (Citrus cinensis) waste: batch and continuous studies. Chem Eng J 155:199–206

38. Gnanasambandam R, Protor A (2000) Determination of pectin degree of esterification by diffuse reflectance Fourier transform infrared spectroscopy. Food Chem 68:327–332

39. Zhang HY, Kan WX, Dong XW, Jiang L, Li ZW, Yang HJ, Cheng HRS (2011) Sorption of methylene blue by carboxymethyl cellulose and reuse process in a secondary sorption. Colloid Surf A Physicochem Eng Asp 380:143–151

40. Zhang WX, Li HJ, Yan H, Jiang ZW, Kan XW, Dong L, Yang H, Li AM, Cheng R (2012) Adsorption of anionic dyes from aqueous solutions using chemically modified straw. Bioresour Technol 117:40–47